EXPERIMENTAL CHARACTERIZATION OF A LARGE APERTURE ARRAY LOCALIZATION TECHNIQUE USING AN SDR TESTBENCH

Marc Willerton, David Yates, Valentin Goverdovsky and Christos Papavassiliou

Department of Electrical and Electronic Engineering
Imperial College London, UK
{marc.willerton05, david.yates, valentin.goverdovsky05, c.papavas}@imperial.ac.uk

ABSTRACT

A software defined radio (SDR) antenna array test bed of independent single channel full duplex radio systems has been constructed using USRP2 boards manufactured by Ettus Research. This provides a flexible platform to easily test the performance of a wide range of array signal processing algorithms at different frequencies and transmission bandwidths with a varying numbers of antennas. Since each channel has its own independent RF chain (including local oscillator), a method to fully synchronize the array elements must be implemented. In addition, array calibration is required to achieve good performance of the array system. In this paper, the implementation of the SDR array platform is described and the practical performance of a recently developed wide aperture array localization algorithm for use in wireless sensor networks (WSN) is evaluated for the first time. Here, large aperture array signal processing techniques are used to locate the position of a signal source operating in the near-far field of the array.

1. INTRODUCTION

Localization of signal sources plays an increasingly important role in many signal processing and communication technologies where spatial information is used to enhance performance and/or provide additional services. For example, knowing the location of a source can allow efficient network optimization algorithms to be performed. Furthermore, localization in itself has many applications in military, industry and research. Some application scenarios for localization include mobile communications, smart antennas, wireless sensor networks and MIMO radar.

A number of localization approaches currently exist. These can be classified as directional and range based approaches. Directional localization approaches estimate the direction of a source with respect to two or more reference points. The intersection of these directions is then found to produce a location estimate. Super-resolution direction finding algorithms such as the well known MUltiple SIgnal Classification (MUSIC) algorithm [1] have a performance which asymptotically increases as a function of SNR$\times L$ where SNR is Signal to Noise Ratio and L is the number of snapshots. Range based approaches estimate the distance between the source and each of the sensors. This may be achieved for example using received signal strength or time of arrival [2]. In this paper, practical results based on a recently developed large aperture array localization approach are presented using an SDR platform. This is an approach based on array processing which has been shown to have an improved performance compared to other approaches by using range and direction [3]. Although the approach is suitable for use in indoor and outdoor environments, in this paper, the experimentation was performed within an anechoic chamber. This allows multipath and other channel effects to be removed. However, in practice, these effects could be contended with via pre-processing in software. This allows the focus of the paper to be placed upon the test bed and the localization algorithm.

In an array processing system, signals received from an array of sensors are processed collectively. This significantly improves the performance compared to that achieved by treating each received signal separately. In a traditional small aperture array system, target localization is often performed assuming the source is present in the far field of the array. It follows that the signal arriving at the array can be treated as a plane wave and that the sensors are all approximately the same distance from the source. Hence, assuming sensors with equal gain, signals received from each sensor will have the same amplitude. However, in a large aperture array, these assumptions no longer hold. The manifold vector must be modified to model a spherical wave propagation which will have amplitude as well as phase dependence on the distance from the source to each sensor in the array. As described in [3], this can be exploited to extract both the magnitude as well as the phase information with respect to the array reference point. Using the array model to process the data from each sensor collectively, traditional problems with range based estimation methods such as noise, transmit power uncertainty and multipath effects as well as sensitivity due to environmental parameters [4] can begin to be overcome using sophisticated array signal processing methods. Currently, no evaluation of the experimental performance of the large aperture array localization algorithm developed in [3] exists

This research was funded by the University Defence Research Centre (UDRC) in Signal Processing (MOD, UK)

in the literature. This paper reports such an evaluation for the first time using a newly developed SDR antenna array test bed.

Low cost Software Defined Radio peripherals are an attractive solution for wireless algorithm development e.g. [5] and [6]. These systems are highly reconfigurable allowing the same hardware to be used in a variety of applications, without requiring specialized systems. An SDR antenna array test bed based on USRP2 boards manufactured by Ettus Research [7] has been developed by the authors at Imperial College London for the purpose of evaluating and developing array processing algorithms for applications such as beamforming, target localization, MIMO and mobile communications. The test bed development work has focused particularly on solving the synchronization and calibration issues associated with using individual transceiver boards as an array. These techniques are explained in this paper.

Practical antenna array systems contain array uncertainties which must be estimated by (pilot or self) array calibration to allow the array signal model to be known. These non-idealities include electrical gain and phase uncertainties of antennas and the RF channel, geometrical uncertainties of antenna locations and mutual coupling effects. Each will lead to degradation in performance of array processing algorithms employed [8] including the algorithm implemented in this paper. In pilot calibration, one or more sources with known parameters (e.g. location) are used to estimate the array uncertainties. An example for a small aperture array is presented in [9]. In self calibration, array uncertainties and unknown source parameters are estimated simultaneously. These tend to be based on an iterative approach. An example for a small aperture array is presented in [10]. It will be shown that an ad-hoc pilot based calibration approach to remove gain uncertainties significantly improves the practical localization performance of the large aperture array system.

In Section 2 the spherical wave array signal model is presented. Next, in Section 3, an overview of the large aperture array localization algorithm developed in [3] is provided. Following this, Section 4 describes the SDR antenna array test bed and experimental setup. In Section 5, it is described how the SDR test bed can be used as a fully synchronized antenna array system by performing phase synchronization. Following this, Section 6 will present experimental results of the localization algorithm implemented on the antenna array test bed and compare these to simulation. Finally, in Section 7, the paper is concluded.

2. SPHERICAL WAVE ARRAY SIGNAL MODEL

Consider a large aperture array of N antennas in the presence of a single source located at a range of ρ with respect to an arbitrary array reference point. Assume the source operates in the near-far field of the array and hence

$$\rho < 2\frac{D^2}{\lambda} \tag{1}$$

where
- D is the array aperture
- λ is the wavelength of the source carrier frequency

The signal vector $\underline{x}(t)$ received by the array can be modeled as

$$\underline{x}(t) = \underline{S}m(t) + \underline{n}(t) \tag{2}$$

In $Equation$ 2, the vector $\underline{S} \triangleq \underline{S}(\theta, \phi, \rho, \mathbf{r}, F_c)$ represents the N-dimensional array manifold vector (array response vector), where θ, ϕ and ρ denote the azimuth, elevation and range of the source with respect to the arbitrary array reference point. Furthermore, F_c is the carrier frequency and $\mathbf{r}$ is a $3 \times N$ matrix containing the Cartesian coordinates of the antennas in the array in meters with respect to the array reference point of the form

$$\mathbf{r} = \left[\begin{array}{ccc} \underline{r}_x, & \underline{r}_y, & \underline{r}_z \end{array} \right]^T \tag{3}$$

In addition, $\underline{n}(t)$ is the complex N-dimensional vector of the noise at the array elements and $m(t)$ is the message of the source which is considered to be slow varying under the definition described in [3]. Since the source operates in the near-far field of the array, a spherical wave array response will be exhibited. Assuming isotropic antennas, this can be expressed [3] mathematically as

$$\underline{S} = (\rho \underline{1}_N \oslash \underline{d})^a \odot \exp\left(-j\frac{2\pi F_c}{c}(\rho \underline{1}_N - \underline{d})\right) \tag{4}$$

where
- a is a constant scalar which represents the path loss exponent
- $\underline{1}_N$ is an N-dimensional column vector of ones
- $\odot$ denotes the Hadamard element by element product operator
- $\oslash$ denotes the Hadamard element by element division operator
- c speed of light $\left(3 \times 10^8 ms^{-1}\right)$

In $Equation$ 4, the vector $\underline{d}$ describes the distance from the source to each of the antennas in the array and can be defined mathematically as

$$\begin{aligned} \underline{d} &= \underline{d}(\theta, \phi, \rho, \mathbf{r}, F_c) \\ &= \sqrt{\rho^2 \cdot \underline{1}_N + \underline{diag}(\mathbf{r}^T\mathbf{r}) - \frac{\rho c}{\pi F_c}\mathbf{r}^T\underline{k}(\theta, \phi)} \end{aligned} \tag{5}$$

where $\underline{diag}(\mathbb{A})$ represents a column vector with elements equal to the leading diagonal of $\mathbb{A}$ and $\underline{k}(\theta, \phi)$ is the wavenumber vector and is defined by the following equation

$$\underline{k}(\theta, \phi) = \frac{2\pi F_c}{c}\left[\cos(\theta)\cos(\phi), \sin(\theta)\cos(\phi), \sin(\phi)\right]^T \tag{6}$$

In this practical study an array of $N = 4$ antennas is employed to attempt to localize a single source. Consider the array reference point to be at the i^{th} antenna. This implies that all the measurements from the array are taken with respect to this antenna. The i^{th} component of the four element array manifold vector is 1 which describes this. Next, consider that the array reference point is changed to lie at each of these

antennas in turn. It is shown in [3] that this will produce four colinear array manifold vector's with different magnitudes as a result of the source being a different distance from each of the array reference points. This property is exploited in the wide aperture localization algorithm.

3. LARGE APERTURE ARRAY LOCALIZATION PROCEDURE

Consider L snapshots of data received from the $N = 4$ antenna large aperture array in the presence of a single source. The signals received over this observation interval can be expressed as the $N \times L$ matrix $\mathbb{X}$ which follows the signal model presented in $Equation$ 2 where

$$\mathbb{X} = \left[\begin{array}{cccc} \underline{x}(t_1), & \underline{x}(t_2), & \cdots & \underline{x}(t_L) \end{array} \right] \tag{7}$$

For the purposes of localization, the array reference point for the matrix $\mathbb{X}$ can be set to the i^{th} antenna by dividing the signals received at each antenna by the signals received at the i^{th} antenna. By rotating the array reference point to be at each of the antennas in the array in turn, four covariance matrices can be constructed as

$$\mathbb{R}_0 = \frac{1}{L}\mathbb{X}_0\mathbb{X}_0^H \tag{8a}$$

$$\mathbb{R}_1 = \frac{1}{L}\mathbb{X}_1\mathbb{X}_1^H \tag{8b}$$

$$\mathbb{R}_2 = \frac{1}{L}\mathbb{X}_2\mathbb{X}_2^H \tag{8c}$$

$$\mathbb{R}_3 = \frac{1}{L}\mathbb{X}_3\mathbb{X}_3^H \tag{8d}$$

where

$$\mathbb{X}_i = \mathbb{X} \oslash (\underline{1}_N \cdot \mathrm{row}_i(\mathbb{X})) \tag{9}$$

Within $Equation$ 9, $\mathrm{row}_i(\mathbb{X})$ denotes the i^{th} row of the matrix $\mathbb{X}$.

In [3], a ratio of ranges between the i^{th} and j^{th} antennas in the array are estimated using the eigenvalues of $\mathbb{R}_i$ and $\mathbb{R}_j$

$$\sqrt[2a]{\frac{\lambda_i}{\lambda_j}} = \frac{\rho_i}{\rho_j} = \kappa_{ij} \tag{10}$$

where ρ_i and ρ_j describe the distance from the source to the i^{th} and j^{th}antennas respectively and λ denotes the so called signal eigenvalues which are found by subtracting the dominant eigenvalue in each of the covariance matrices with the average of the remaining eigenvalues.

Using $Equation$ 8 and letting antenna 0 be the global reference antenna, the ratio of range between the remaining antennas and this antenna creates three κ values

$$\kappa_1 = \sqrt[2a]{\frac{\lambda_1}{\lambda_0}} \tag{11a}$$

$$\kappa_2 = \sqrt[2a]{\frac{\lambda_2}{\lambda_0}} \tag{11b}$$

$$\kappa_3 = \sqrt[2a]{\frac{\lambda_3}{\lambda_0}} \tag{11c}$$

Using the array geometry, these values correspond to different circular loci with centers and radii described by

$$\underline{r}_{c_1} = \frac{1}{1-\kappa_1^2} \cdot \underline{R}_1 - \frac{\kappa_1^2}{1-\kappa_1^2} \cdot \underline{R}_0 \tag{12a}$$

$$R_{c_1} = \left| \frac{\kappa_1}{1-\kappa_1^2} \right| \cdot \|\underline{R}_0 - \underline{R}_1\| \tag{12b}$$

$$\underline{r}_{c_2} = \frac{1}{1-\kappa_2^2} \cdot \underline{R}_2 - \frac{\kappa_j^2}{1-\kappa_j^2} \cdot \underline{R}_0 \tag{12c}$$

$$R_{c_2} = \left| \frac{\kappa_2}{1-\kappa_2^2} \right| \cdot \|\underline{R}_0 - \underline{R}_2\| \tag{12d}$$

$$\underline{r}_{c_3} = \frac{1}{1-\kappa_3^2} \cdot \underline{R}_3 - \frac{\kappa_3^2}{1-\kappa_3^2} \cdot \underline{R}_0 \tag{12e}$$

$$R_{c_3} = \left| \frac{\kappa_3}{1-\kappa_3^2} \right| \cdot \|\underline{R}_0 - \underline{R}_3\| \tag{12f}$$

where
- $\underline{r}_{c_j}$ is the center of the j^{th} locus in Cartesian coordinates
- R_{c_j} is the radius of the j^{th} locus
- κ_j is the κ associated with the j^{th} locus
- $\underline{R}_j$ denotes the j^{th} antenna location in Cartesian coordinates
- $\underline{R}_0$ denotes the location of the global reference antenna in Cartesian coordinates

The intersection of these loci provides an estimate of the source location.

4. SDR ARRAY TESTBED SETUP

Traditional array systems involve RF hardware which consumes large amounts of Size, Weight and Power (SWAP). These systems tend to be inflexible, operating within a given frequency band and supporting a limited number of antennas in certain fixed configurations. They also tend to perform a limited number of tasks. The advent of Software Defined Radio (SDR) aims to convert hardware design problems into software and at the same time reduce SWAP, increase system flexibility and reduce cost. Here, signals are converted from digital to analogue (and visa-versa) at the front end of the system using software defined peripheral boards. These tend to be basic devices which allows powerful signal processing to be carried out in software. The Universal Software Radio Peripheral 2 (USRP2) board manufactured by Ettus Research is one of these devices. These boards contain support for up to two (but usually one) full duplex channels with a bandwidth of up to $50MHz$. They are small $(20.2 \times 15.8 \times 4.8)\ cm$ and light $(< 1\ kg)$ devices which can easily be interfaced with a computer using a gigabit Ethernet connection and consume a DC power of $18W$. The carrier frequency can be changed easily by swapping their daughterboards. A full specification of the boards can be found in [7]. The USRP2 boards can be used with GNURadio [11], an open source software environment which can be used to configure the

boards to operate with a certain carrier and gain and perform the signal processing.

Several USRP2 boards must be fully synchronized to form the antenna array system. However, each board contains its own local oscillator locked to its own reference signal which will cause phase drift between channels. Furthermore, samples are referenced based on a timestamp value set independently from the host PC in the FPGA which will cause misalignment of samples collected at the same time in different boards. For many array processing applications, it is assumed that the same local oscillator and time reference exists between antennas. However, having this restricts the flexibility of the system. This problem can be solved in part by providing a common $10MHz$ clock reference signal and a 1 PPS (Pulse Per Second) signal to each of the boards. The former provides a reference for the USRP2 system clock which also provides the reference for the local oscillator. This will allow the local oscillator on each board to be tuned to the same frequency giving a frequency synchronized system. The later is used to reset the timestamp value on each board at the rising edge of the PPS signal when the boards are initialized. However, this alone is not enough to form a fully synchronized array system. In addition, the system must be phase synchronized. This problem will be discussed in Section 5 and a solution will be provided.

For the purposes of this paper, an array receiver of $N = 4$ antennas was constructed using four USRP2 boards with RFX2400 daughterboards (operating range: $2.3 - 2.9GHz$). Each board was connected to a common $10MHz$ clock reference signal and a 1 PPS signal. Data was transferred to the host computer for processing via gigabit Ethernet switch under a sampling rate of $1,562,500$ $samples/second$ in each channel and an operating frequency of $2.43GHz$ was chosen for the system. The source whose location is to be estimated consisted of a single USRP2 board transmitting a $100KHz$ sine wave amplitude modulated on a $2.43GHz$ carrier signal at a power of $17dBm$. Omnidirectional monopole antennas were used. The large aperture measurements were carried out in an anechoic chamber to eliminate the effects of multipath. This allows a direct comparison with the theoretical predictions in terms of RMS error versus the signal-to-noise ratio (SNR) multiplied by the number of snapshots (L), which were made in [3].

5. ARRAY SYNCHRONISATION

In Section 4, it was shown how the USRP2 boards are particularly suitable for use in a flexible multi-antenna environment by using a common clock reference and PPS signal to each of the boards. The clock reference signal provides a reference to lock the local oscillators in each board which prevents phase drift. However, frequency synchronization is not enough for a true array system. In addition, phase synchronization is also required. This is not achieved using the clock reference signal due to a phase ambiguity in the implementation caused by a division of the $100MHz$ clock by 16 to give a reference frequency of $6.25MHz$ to which the RF local oscillator is locked. Each time a retune command is sent, the phase between channels changes because of this ambiguity. For applications such as localization, in which the channel phase difference can be key, this problem would have to be compensated for each time a new set of data is collected. It has been found that the second RF channel (RF2) can be used for estimating the phase ambiguity. By applying a common $2.43GHz$ carrier only tone directly into the RF2 port of each USRP2 board in the array, the phase between channels can be synchronized by introducing phase weightings to align the signals received at the array from the carrier only tone on top of each other. The desired over the air signal can then be isolated by digital filtering in software (ensuring the over-the-air signal doesn't operate too close to DC at baseband) and the weightings can be applied to this signal to remove the phase ambiguity. The reference tone is provided by another USRP2 board. This process is illustrated in $Figure$ 1 showing the alignment of the phase of the carrier only tone.

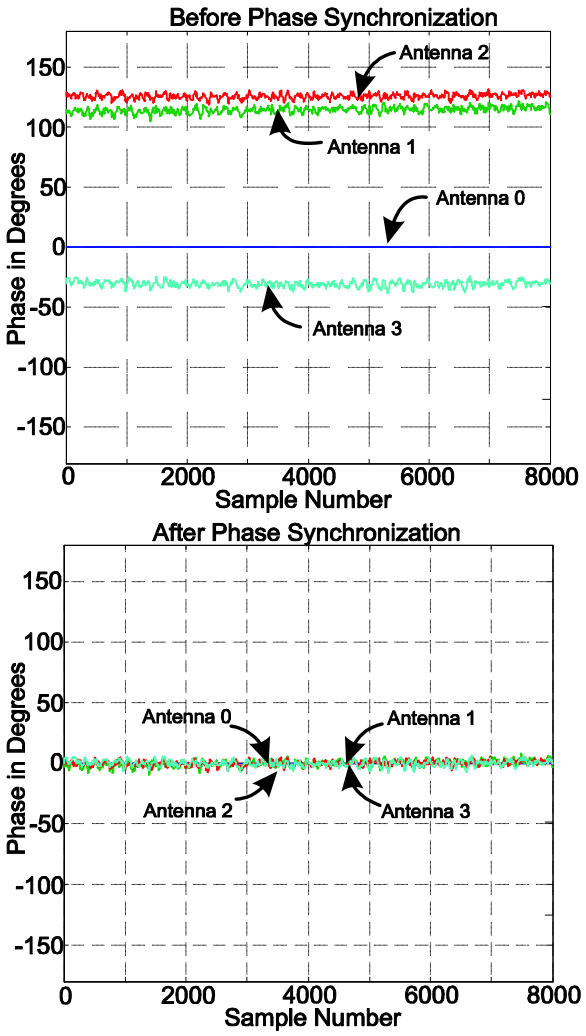

Fig. 1. Implementation of phase synchronization using a carrier only tone

Having solved the phase ambiguity problem, the test bench can now form a true array system. $Figure$ 2 shows the full array test bench setup used with the reference clock, PPS signal and the $2.43GHz$ carrier only tone.

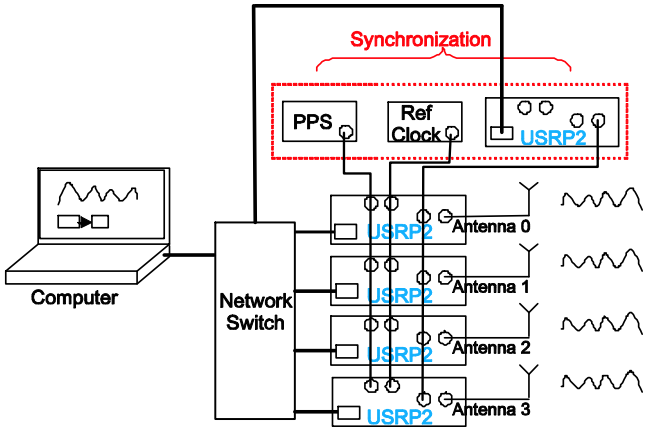

Fig. 2. Array testbench setup comprising of 4 antennas/USRP2 boards

6. EXPERIMENTAL RESULTS

A fully synchronized large aperture array of $N = 4$ antennas was constructed with the geometry shown in $Figure$ 3 with a single signal source transmitting at $F_c = 2.43GHz$ whose location is to be estimated.
Details of the experimental setup are provided in Sections 4 and 5. The array based localization algorithm described in Section 3 is implemented using $L = 100$ snapshots. This provides three loci where the estimate of the source location is taken to be at the centroid of the triangular shape created by the intersection of the loci. Results are illustrated in $Figure$ 4 under an SNR of approximately 35.14 dB.

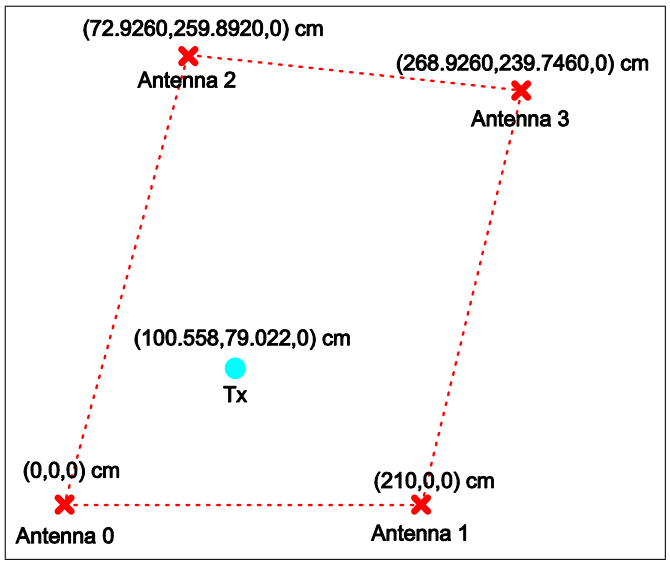

Fig. 3. Large aperture array geometry experimental setup

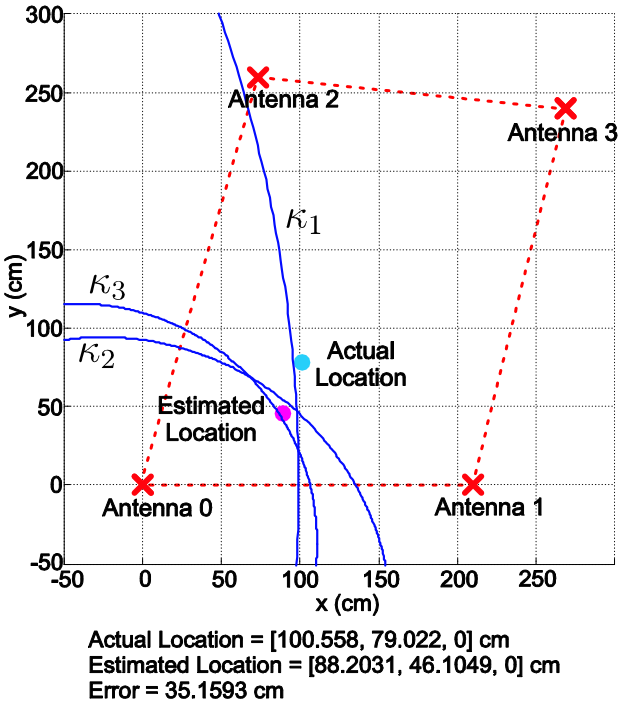

Fig. 4. Practical result of the large aperture array localization procedure for the unknown Tx location using $L = 100$ snapshots under measured SNR=35.14 dB with the setup in $Figure$ 3

This provides an estimation error of 35.1593 cm. In contrast, a simulation study for this experimental setup under the same SNR and number of snapshots provides an estimation error of just 9.0203 cm as illustrated in $Figure$ 5.
Results show that the simulated performance far exceeds the practical in terms of the estimation error. Furthermore, the intersection points of the three loci are also at a more common location creating a smaller triangular area from which the location estimate is calculated. It is clear that κ_2 and κ_3 are incorrectly centred or have an incorrect radius. Array uncertainties within the array signal model will cause these effects and should be accounted for. For the purposes of this study it will be assumed that these are predominantly due to gain uncertainties present in the array.

Consider a single pilot source present at a known location within the array as illustrated in $Figure$ 6. By rotating the array reference point, κ_1, κ_2 and κ_3 can be found for the pilot source. In the presence of no uncertainties, multiplying these by the distance between the pilot source and antenna 0 (the global array reference point) should provide an estimate of the distance between the pilot source and antennas 1, 2 and 3. However, in the presence of gain uncertainties, these values will be incorrect. Knowing the actual distances between the pilot source and each of these antennas, modifications can be made to the gain of the signals received at the antennas 1, 2 and 3 to modify κ_1, κ_2 and κ_3 respectively so that the estimate of distance is correct. The scaling factor values detailed in $Table$ I are found to provide the modifications required. Applying

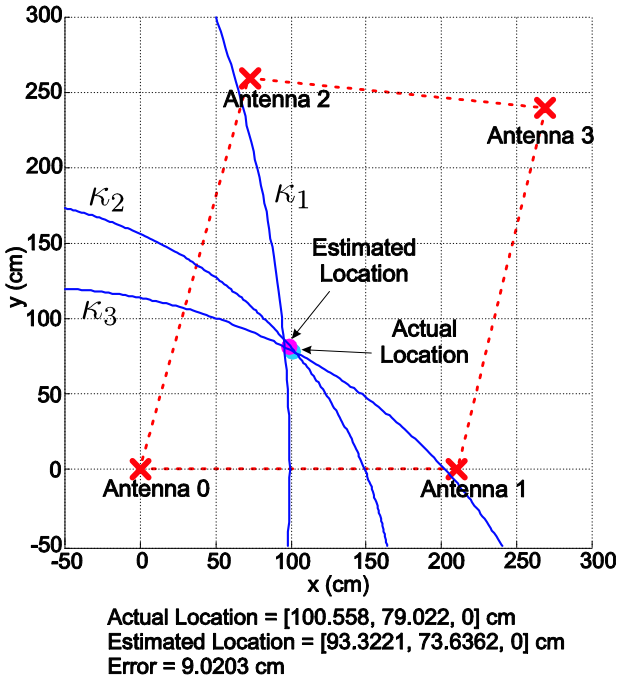

Fig. 5. Simulated result of the large aperture array localization procedure for the unknown Tx location using $L = 100$ snapshots under SNR=35.14 dB with the setup in *Figure* 3

these scaling factors to estimate the location of the unknown source as detailed in *Figure* 3, the result of the localization algorithm is illustrated in *Figure* 7.

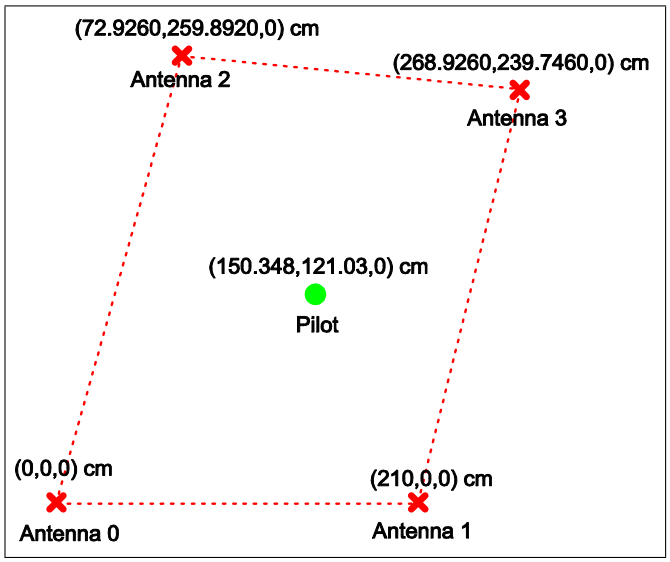

Fig. 6. Large aperture array geometry in the presence of a pilot source

Following the calibration procedure, the localization error is now just 6.0996 cm which shows a significant improvement compared to the uncalibrated case. In terms of the error figure alone, the performance in this case exceeds that found in the simulation study. However, it is clear from comparing

Antenna	Expected $\underline{d}$ in cm	Calculated $\underline{d}$ in cm	Scaling Factor
0	193.0000	193.0000	1.0000
1	135.0000	114.8646	0.8508
2	159.0000	197.7393	1.2436
3	168.0000	264.9428	1.5770

TABLE I
ACCOUNTING FOR SENSOR GAIN UNCERTAINTIES IN THE ARRAY

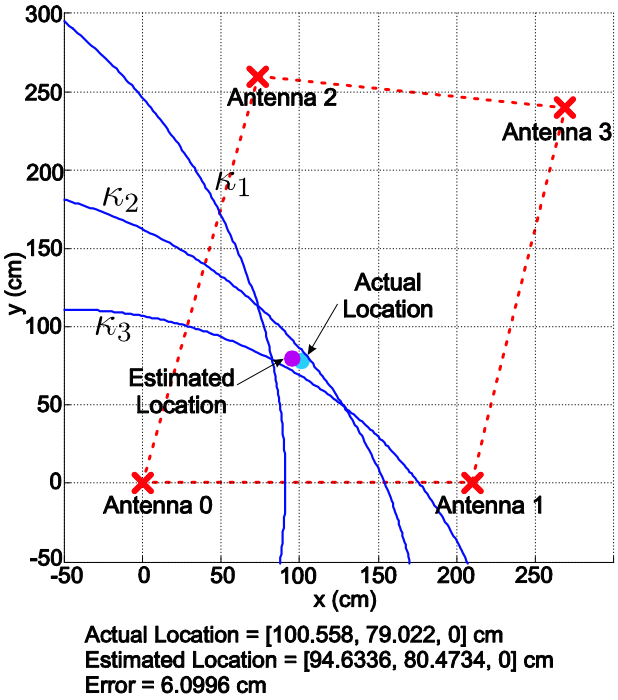

Fig. 7. Practical result of the large aperture array localization procedure after calibration for the unknown Tx location using $L = 100$ snapshots under measured SNR=35.14 dB for the setup in *Figure* 6

Figures 5 and 7, that the practical result still has large distances between pairs of intersecting loci resulting in a large triangular shape area being produced. This reduces the reliability of the array centroid method used to estimate the location of the source. Its presence implies location dependant array uncertainties are present such as antenna location which should be removed to further improve the result.

7. CONCLUSION

The results illustrated in this paper show that a collection of individual USRP2 units can be successfully synchronized using a common clock reference, PPS and carrier signal to form an antenna array system. This provides a test bed which is readily expandable, works over a large range of frequencies and where the practical performance of array processing algorithms can easily be tested. It will therefore provide a useful platform to test a wide variety of array processing algorithms for use in different applications. The results of the

large aperture array localization procedure clearly show a good performance compared to simulation studies following basic calibration attempts. However, a more sophisticated approach which includes the estimation of antenna location uncertainties will likely see the performance being improved even further. Next the performance of the algorithm and test bed must be investigated outside the anechoic chamber. This will assist in highlighting the additional problems which must be overcome for the system to operate in more realistic scenarios.

REFERENCES

[1] R. Schmidt, "Multiple emitter location and signal parameter estimation," *IEEE Transactions on Antennas and Propagation*, vol. 34, no. 3, pp. 276–280, Mar. 1986.

[2] N. Patwari, J. Ash, S. Kyperountas, A. Hero, R. Moses, and N. Correal, "Locating the nodes: cooperative localization in wireless sensor networks," *IEEE Signal Processing Magazine*, vol. 22, no. 4, pp. 54–69, Jul. 2005.

[3] A. Manikas, Y. Kamil, and P. Karaminas, "Positioning in Wireless Sensor Networks Using Array Processing," *Global Telecommunications Conference, 2008. IEEE GLOBECOM 2008. IEEE*, pp. 1 – 5, 2008.

[4] K. Whitehouse, C. Karlof, and D. Culler, "A practical evaluation of radio signal strength for ranging-based localization," *ACM SIGMOBILE Mobile Computing and Communications Review*, vol. 11, no. 1, p. 41, Jan. 2007.

[5] R. C. Qiu, Z. Chen, N. Guo, Y. Song, P. Zhang, H. Li, and L. Lai, "Towards a Real-Time Cognitive Radio Network Testbed: Architecture, Hardware Platform, and Application to Smart Grid," in *2010 Fifth IEEE Workshop on Networking Technologies for Software Defined Radio Networks (SDR)*. IEEE, Jun. 2010, pp. 1–6.

[6] J. M. V. Burgos, E. Gago-Cerezal, V. A. Gracia, and L. M. C. Cervera, "DEMIURGO, an SDR Testbed for Distributed MIMO," in *2006 3rd International Symposium on Wireless Communication Systems*. IEEE, Sep. 2006, pp. 210–213.

[7] Ettus Research, "USRP2 Product Overview." [Online]. Available: http://www.ettus.com/downloads/ettus_ds_usrp2_v5.pdf

[8] A. Swindlehurst and T. Kailath, "A performance analysis of subspace-based methods in the presence of model errors. I. The MUSIC algorithm," *IEEE Transactions on Signal Processing*, vol. 40, no. 7, pp. 1758–1774, Jul. 1992.

[9] N. Fistas and A. Manikas, "A new general global array calibration method," in *Proceedings of ICASSP '94. IEEE International Conference on Acoustics, Speech and Signal Processing*. IEEE, 1994, pp. IV/73–IV/76.

[10] A. Weiss and B. Friedlander, "Array shape calibration using sources in unknown locations-a maximum likelihood approach," *IEEE Transactions on Acoustics, Speech, and Signal Processing*, vol. 37, no. 12, pp. 1958–1966, 1989.

[11] GNURadio Home Page, "GNURadio." [Online]. Available: http://gnuradio.org/